The Odden ice feature of the Greenland Sea and its association with atmospheric pressure, wind, and surface flux variability from reanalyses

Jeffrey C. Rogers[1] and Meng-Pai Hung[1]

Received 7 December 2007; revised 11 March 2008; accepted 26 March 2008; published 26 April 2008.

[1] The Odden sea ice feature of the Greenland Sea is identified in a rotated principal component analysis of Hadley Center winter sea ice concentration data extending from 1951–2005. Time series of the Odden ice extent are evaluated in the context of sea level pressure, surface wind, air temperature, cloud, and energy flux variations using NCEP-NCAR reanalyses. Odden was a recurring feature in winters 1966–1972, during the Great Salinity Anomaly (GSA), and appeared occasionally in the 1980s and 1990s but has occurred rarely since 2000. Odden formation is associated with northernmost Atlantic high pressure, a negative North Atlantic Oscillation, and anomalous westerly winds. Its formation is most highly correlated, however, to air temperature and fluxes of sensible/latent heat, and downward longwave radiation. Air temperature and downward longwave flux anomalies in the preceding autumn are also unusually low in advance of a winter Odden ice cover while heat fluxes are weakly positive. All parameters, including the ice cover anomaly, exhibit significant winter to winter persistence over time. **Citation:** Rogers, J. C., and M.-P. Hung (2008), The Odden ice feature of the Greenland Sea and its association with atmospheric pressure, wind, and surface flux variability from reanalyses, *Geophys. Res. Lett.*, *35*, L08504, doi:10.1029/2007GL032938.

1. Introduction

[2] The Odden is a large tongue of sea ice that builds northeastward into the Greenland Sea during winter months, typically occurring between 8°W and 5°E and between 73° and 77°N [*Shuchman et al.*, 1998]. At its maximum extent the Odden sea ice feature may cover 250,000 km^2 to 330,000 km^2 [*Wadhams and Comiso*, 1999; *Comiso et al.*, 2001], and it can rapidly expand or shrink over a period of a few days. In some winters it persists for months, while failing to form in others. In some years Odden appears as a northeastward protruding ice tongue, with a bay of open water (the Nordbukta) lying between it and the coastal east Greenland pack ice, while in heavy ice years the Nordbukta fills with ice and the Odden appears as a bulge extending eastward from the east Greenland ice [Wadhams and Comiso, 1998; *Comiso et al.*, 2001, Plate 3]. Interannual Odden ice extent variability is important as it affects winter convection in the Greenland Sea through salt flux [*Shuchman et al.*, 1998; *Toudal and Coon*, 2001]. Odden sea ice formation and decay is dependent on meteorological [*Shuchman et al.*, 1998] and oceanographic parameters such as the strength of the Jan Mayen Current and ocean bathymetry [*Comiso et al.*, 2001]. Meteorologically, interactions between air temperature anomalies, wind direction and speed, and ocean pre-conditioning play an important role in Odden formation and decay on weekly and daily time scales [*Visbeck et al.*, 1995; *Shuchman et al.*, 1998; *Toudal*, 1999; *Comiso et al.*, 2001].

[3] *Deser et al.* [2000] and *Chasmer and LeDrew* [2001] recently demonstrate the usefulness of principal component analysis in sea ice concentration (SIC) analyses. The objective of this paper is to expand upon *Deser et al.*'s [2000] study by quantitatively defining Odden events in northern Atlantic/Arctic SIC data for 1951–2005 from rotated principal component analysis. The time series coefficients of the Odden component will be used to evaluate the pressure, wind field and energy flux variability associated with the Odden using NCAR-NCEP reanalyses (NNR). The analyses identify long-term statistical linkages between physical mechanisms and the Odden ice extent, expanding on meteorological analyses by *Shuchman et al.* [1998] and *Comiso et al.* [2001] and seek to improve our physical understanding of links between the Odden and the atmosphere.

2. Data and Methods

[4] We use the Hadley Center Sea Ice and Sea Surface Temperature (HadISST) [*Rayner et al.*, 2003] SIC fields on a 1° × 1° grid from 1951–2005 (N = 55), available from the Hadley Center Meteorological Office. Winter ice concentrations are averages of middle of the month (D-J-F) SIC fields at grid points from 45° to 90°N, and from 90°W to 90°E, and dated as the year of the January. The main HadISST ice data source prior to 1978 is the *Walsh* [1978] Northern Hemisphere end of month SIC charts that drew upon data from several sources and which were adjusted in making mid-monthly HadISST SIC fields [*Rayner et al.*, 2003]. Starting in October 1978 the HadISST SIC data rely primarily on Scanning Multichannel Microwave Radiometer (SMMR), and the Special Sensor Microwave Imager (SSM/I) passive microwave satellite data. Monthly mean SLP, air temperature, and 6-hourly near surface u- and v-component geostrophic wind speeds were obtained from the NNR data [*Kalnay et al.*, 1996]. Monthly mean cloud cover, and fluxes of latent/sensible heat and downward longwave radiation are also based on 6-hourly data. *Deser et al.* [2000] have shown that NNR surface fluxes are large and qualitatively accurate along the winter Greenland sea ice margins during extreme events. Lag 1 autocorrelations (r_1) are determined for data parameters and are incorporated

[1]Atmospheric Science Program, Department of Geography, Ohio State University, Columbus, Ohio, USA.

0094-8276/08/2007GL032938$05.00

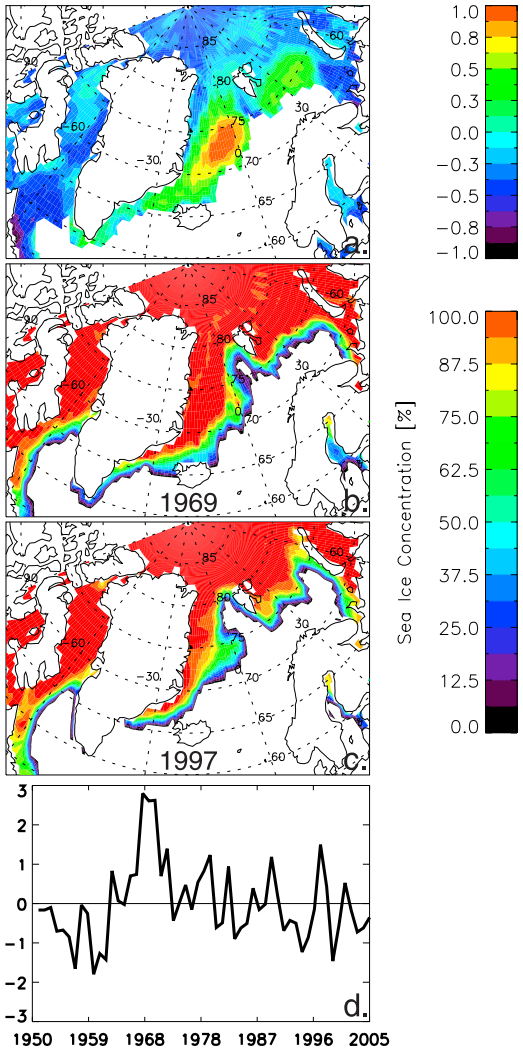

Figure 1. (a) The magnitude of the HadISST RPC4 winter spatial loadings of Atlantic Arctic 1951–2005 sea ice concentration (SIC) and (d) their time series. The January mid-monthly SIC in (b) 1969, and (c) 1997.

into tests of correlation between 2 variables (e.g., x, y) by using a lower effective number of degrees of freedom (N_{eff}) through $N_{eff} = N\left(\frac{1-r_{1x}r_{1y}}{1+r_{1x}r_{1y}}\right)$.

[5] Rotated Principal Component Analysis (RPCA) identifies the simple regional structures that exist in winter SIC fields as well as their associated time series. Initially 4 empirical orthogonal functions (EOFs; unrotated components) are obtained, each explaining a minimum 5%, and collectively 66.1% of the total SIC dataset variance. The first HadISST EOF (not shown) is nearly identical to that of *Deser et al.* [2000, Figure 3], exhibiting a longitudinal SIC dipole between areas west of Greenland and those around the Barents Sea, and it explains 40% of the dataset variance. Rotation of the variance contained in the 4 EOFs removes the constraint that they be orthogonal to EOF 1 and rotated patterns instead identify the simple, unique, regional patterns of spatial variability occurring within the SIC dataset. The result yields 4 RPCs, each again explaining at least 5% of the rotated dataset variance. This paper focuses only on RPC4, which exhibits large SIC variability in the Odden region (see Results) and explains 19.1% of the northern Atlantic/Arctic SIC variability (second largest percent) after rotating the EOFs.

3. Results

[6] Winter RPC4 (Figure 1a) exhibits largest SIC variability over a southwest/northeast oriented area between 15°W and 5°E, and between 70° and 76°N with loading values declining sharply toward the eastern coast of Greenland. This variability center is the spatial domain of the Odden sea ice feature. Odden ice concentrations are weakly in phase (Figure 1a) with those of the east Greenland current south of 75°N to Iceland, as well as to a large area southeast of Svalbard in the northern Barents Sea. Odden SIC variability is otherwise out-of-phase with (i) an area southwest of Svalbard, (ii) the northern East Greenland Current mostly north of 75°N including Fram Strait, and (iii) the Davis Strait/Labrador Sea area southwest of Greenland.

[7] Time series variability of the Odden RPC4 (Figure 1d) is characterized by positive values in 1979, 1982, 1986, 1989, 1997 and 1998, representing known high Odden ice concentration winters [*Comiso et al.*, 2001; Plate 7; *Shuchman et al.*, 1998, Figures 3a, 3b]. Conversely, low negative scores of 1983–1985 and 1991–1993 correspond to weak, little-persistent Odden events and the minima in 1994 and 1995 correspond to winters when Odden virtually failed to appear in passive microwave records. The largest positive score values (> +2.0) occur during 1968–1970, when the Great Salinity Anomaly (GSA) peaked in the East Greenland Sea [*Dickson et al.*, 1988] and scores are generally high from 1966–1972. Very lowest negative scores cluster from 1960–1962, before the GSA, and do not recur until 1994 and 1999.

[8] Comparison of mid-January HadISST SICs (Figures 1b and 1c) for 1969 and 1997 (the strongest recent Odden) shows similar eastward sea ice extents and both months seem to be bulge events, although Nordbukta did occur in some months in 1997. January 1969 otherwise has much heavier SIC along coastal Greenland and the westernmost Odden domain, while Davis Strait is largely free of ice in both Januaries.

[9] Mean winter SLP fields are obtained during the 12 highest positive Odden events (Figure 2a), and the 12 lowest negative ("non-Odden") events (Figure 2b) during 1951–2005. Non-Odden winters have a mean Icelandic low around 995 hPa, which is lower than that (1001 hPa) during Odden years. The SLP departures exceed +3 hPa (from the 55-winter mean) over the Odden area during Odden winters (Figure 2c) and the anomalous high pressure dominates most of the northernmost Atlantic and environs. Non-Odden winters are characterized (Figure 2d) by anomalous low SLP (under -3 hPa) over most of the northernmost Atlantic. Mean anomalous near-surface geostrophic winds inferred from the SLP departure fields suggest that the Odden events (Figure 2c) are dominated by more divergent high pressure than usual while non-Odden events are characterized by an intensified easterly flow toward Greenland around a deep Icelandic Low. The mean winter pressure difference (Figure 2e), Odden minus non-Odden, is largest over the

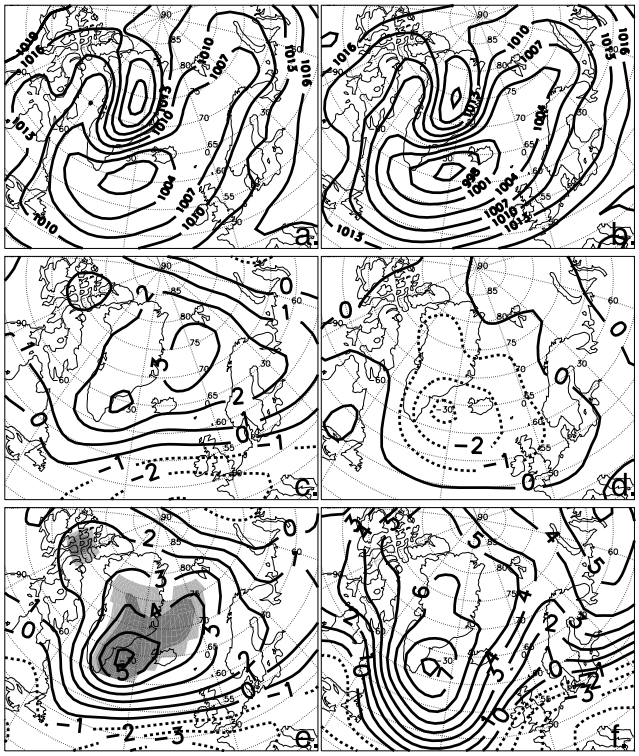

Figure 2. Mean winter sea level pressure (3 mb intervals) for (a) 12 Odden years, and (b) 12 Non-Odden years with highest and lowest RPC scores since 1951. Mean SLP anomalies (1 mb intervals) from the 1951–2005 mean for (c) Odden, and (d) Non-Odden years. (e) Mean winter SLP differences, Odden minus non-Odden with shading intervals defining the 95% and 99% confidence intervals from a two-tailed t-test. Positive (negative) differences are solid (dashed). (f) Like Figure 2c but for the mean SLP departures for winters 1968–1970 from the 1951–2005 average.

Denmark Strait but positive differences over 4 hPa extend over the Odden ice feature area and are statistically significant using a two-tailed t-test. These results indicate a link to the North Atlantic Oscillation (NAO), the index of which (updated from *Rogers* [1984]) is correlated r = −0.38 (N_{eff} = 39; 95% confidence) to the Odden (Figure 1d). N_{eff} is based on one winter r_1 values of +0.53 and +0.32 for the Odden scores and NAOI, respectively.

[10] Large positive mean SLP anomalies (Figure 2f) occur broadly across Greenland and the northeastern Atlantic during winters 1968–1970. The unusually large high pressure anomaly exceeds +8 hPa near the Denmark Strait and +5 hPa over the Odden area. Anomalous anticyclonic flow around this center would substantially weaken the normal polar easterly flow typically occurring north of the Icelandic Low. Positive pressure departures during 1968–1970 (Figure 2f) exceed those of Figure 2c for the 12-case average.

[11] Frequency histograms (Figure 3a) of the mean winter SLPs averaged over longitudes 5°W to 5°E at 75°N are made using 15 Odden and 19 non-Odden winters having scores (Figure 1d) exceeding absolute 0.5. The majority of non-Odden winters have pressures between 996 hPa and 1008.5 hPa, with none exceeding 1012.2 hPa, while most

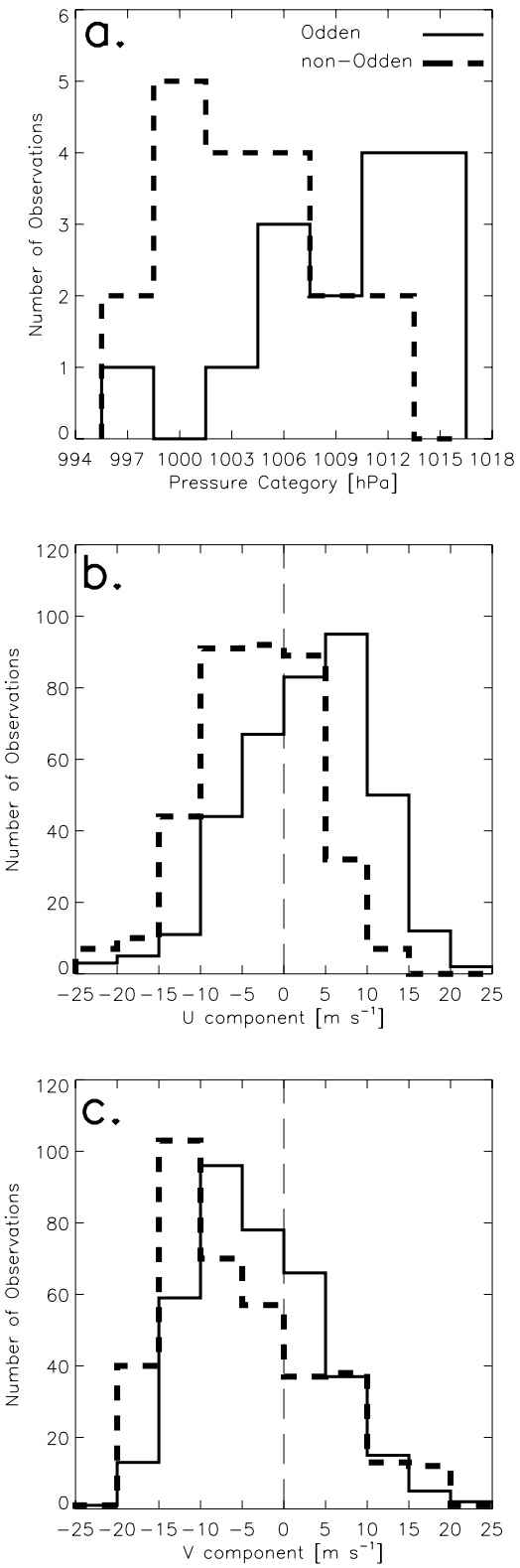

Figure 3. Frequency histograms of (a) mean winter Odden-area SLP along 75°N, and observations in 3 Januaries each of (b) u-component winds and (c) v-component winds, for Odden (solid) and non-Odden (dashed) cases.

Table 1. Correlations Between the Winter Odden Time Series Scores and NNR Temperature, Cloud, and Flux Parameters for the Concurrent Winter, and the Preceding Autumn and Winter[a]

	DJF_0	SON_{-1}	DJF_{-1}	NAOI	DJF r_1
Air Temperature	***−0.79***	**−0.60**	***−0.47***	**+0.49**	***+0.46***
Total Cloud	***−0.69***	−0.28	**−0.32**	**+0.57**	+0.24
Latent Heat Flux	***−0.69***	+0.24	**−0.36**	+0.30	***+0.41***
Sensible Heat Flux	**−0.63**	**+0.38**	**−0.33**	+0.20	**+0.35**
Downward LWF	***−0.82***	**−0.56**	***−0.45***	**+0.54**	***+0.36***

[a]LWF = longwave flux. SON_{-1} is autumn and DJF_{-1} is winter. NAO index coefficients are correlations with the concurrent parameter values during DJF_0. Coefficients that are statistically significant with 95% (99%) confidence, after determining N_{eff} based on time series lag 1 autocorrelations (r_1) among winters (shown in the far right column), are indicated in bold (bold italics).

Odden events have pressures above 1004.5 hPa. The seasonal mean pressures along 75°N of these histograms are correlated r = +0.90 to Denmark Strait SLP between 60°–65°N (the normal center of the Icelandic Low).

[12] Wind speed component (u and v) frequencies are obtained for 3 Odden and 3 non-Odden Januaries using 372 (31 days × 4 obs × 3 Januaries) 6-hourly reanalysis observations (Figures 3b and 3c). These sample Januaries are based on *Shuchman et al.* [1998] and *Comiso et al.*'s [2001] data, cited earlier, regarding overall mid-winter large (or very small) Odden ice extents. Westerly (+u) winds (Figure 3b) between 0 and +10 ms^{-1} are the two most frequent wind categories during Odden Januaries (1979, 1982, 1997) while winds are dominantly easterly (−u) between 0 and −10 ms^{-1} during non-Odden Januaries (1984, 1994, 1995). The dominant meridional v-component flow (Figure 3c) is northerly (−v) in both Odden and non-Odden Januaries, although southerly (+v) winds can also occur. Thus Odden Januaries tend to have frequent northwesterly while non-Odden have mostly northeasterly flow.

[13] Mean monthly values of five other NNR parameters are seasonally averaged at grid points over the Odden region and correlated to both the HadISST Odden time series and the NAO index (Table 1). Regional air temperature, heat fluxes, cloud cover, and downward longwave fluxes are negatively correlated to the winter Odden time series (Figure 1d), indicating that below normal DJF_0 values (column 1) for each occur during high Odden ice events (Table 1), and conversely. Winter latent and sensible heat fluxes are highly correlated with each other (r = 0.97) over the 55 winters as are air temperature and downward longwave flux (r = 0.93). Evaluation of stepwise regression models (not shown) indicate that the highest r^2 with the Odden time series occurs with a combination of either downward longwave flux and latent heat flux or longwave flux with sensible heat (both have r^2 = .75). These combinations were slightly better than those of air temperature with the heat fluxes (r^2 = .71) in estimating the Odden ice index value. The winter NAOI (column 4) is best correlated to the concurrent cloud cover but has no significant link to latent and sensible heat fluxes. Column 5 (Table 1) is the lag 1 autocorrelation (r_1), indicative of the winter-to-winter persistence in these parameters.

[14] Air temperature and downward longwave flux in the preceding autumn (SON_{-1}; column 2) are also significantly correlated to DJF Odden ice extent (Table 1); peaking seasonally in November in the individual monthly data (not shown). Autumn latent and sensible heat flux correlations are low but positive, suggestive of autumn heat loss during low autumn temperatures and prior to winter Odden ice formation, and their correlations peak in October (not shown) before becoming negative in winter. Correlations of fluxes in the preceding winter (DJF_{-1}; column 3) to the current DJF_0 ice conditions are highest of any season outside of SON_{-1} and are likely linked to the r_1 values (Table 1) representing significant persistence among winters in each parameter except cloud cover.

4. Discussion

[15] The Odden sea ice feature emerges here as the second most important SIC spatial variability pattern in the Atlantic Arctic, accounting for 19.8% of the rotated variance. The most extreme Odden SIC maxima occur in 1968–1970 (Figures 1b and 1d) during the Great Salinity Anomaly, which was associated with high pressure over the northern Atlantic [*Dickson et al.*, 1988; Figure 4], just as we show the Odden to be (Figure 2). Northern Atlantic mean winter SLP steadily decreases after 1972 [e.g., *Dickson et al.*, 2000, Figure 1b] and Odden events become more infrequent.

[16] The analyses here elaborate on the key differences in both regional pressure and wind fields that affect the occurrence of Odden, using long-term data, and they show that the NAO correlation to Odden ice extent is small but negative (r = −0.38). Previous papers [*Shuchman et al.*, 1998; *Comiso et al.*, 2001] identified positive NAO/Odden ice extent correlations of r ≈ +0.40, which were not reproducible here. Comiso does subsequently describe an example of the Odden/NAO association (see Figures 2b and 2d above), linking unusually low pressure around Iceland and associated easterly winds north of Iceland during low Odden ice extent. However, while the Icelandic pressure anomaly and Odden ice are directly in phase (e.g., low pressure = low ice, and conversely), the sign of the NAO index is always opposite that of Icelandic regional SLP. Figure 1a further illustrates the inverse NAO link to Odden ice extent, indicating that Odden ice extent is out-of-phase with that of the Davis Strait. Some extreme events support this as Davis Strait had below normal ice cover in Januaries of 1969 and 1997 (Figures 1b and 1c) and it had extraordinarily severe ice in the winters 1983 and 1984 [*Rogers et al.*, 1998; Figure 4] when the Icelandic low was unusually deep (NAO+) and Odden was very weak to non-existent.

[17] The physical parameters in Table 1 are much more directly linked to Odden ice extent than the NAO pressure

field indicator, and the NAO made no additional significant contribution to stepwise regression models of the Odden index. Whereas air temperature and downward longwave flux are correlated about $r \approx -0.8$ to Odden ice extent (Table 1), the NAOI is only correlated $r \approx +0.5$ to those parameters and has an even lower direct correlation to the Odden ice ($r = -0.38$). Anomalous high pressure around Iceland and the Odden region likely induces clear skies and low air temperatures during Odden, in agreement with observations by *Shuchman et al.* [1998] and *Comiso et al.* [2001] that Odden forms thermodynamically in cold air outbreaks. Higher than normal SLP can also create increasingly frequent westerly flow as shown in 6-hourly reanalysis data for a sample of 3 well-defined Odden Januaries (Figure 3b), and this flow likely remains cold as it traverses sea-ice covered ocean on the way to the Odden region. *Wadhams and Comiso* [1999] show that older multiyear sea ice can also be advected eastward out of the East Greenland Current, a process they identify primarily with spring and summer Odden region ice cover and consistent with continuing westerly advection. *Shuchman et al.* [1998, Figure 4] also associated westerly winds with Odden growth periods and showed that northerly winds lead to Odden decay. While our Figure 3c agrees that northerlies prevail in non-Odden Januaries, the big difference is the dominance of easterly winds in non-Odden months (Figure 3b). Finally, the results indicate a large degree of persistence in the data going into winter. Persistence occurs in the Odden ice extent itself (winter to winter $r_1 = +0.53$), the NAO, air temperature, and the energy flux parameters (Table 1), suggestive of some potential predictability of Odden winter ice events. Autumn air temperatures and downward longwave flux also have a sizeable negative correlation to winter ice and are potentially related weakly to positive fluxes of latent and sensible heat in that preceding season. Coupled ocean-atmosphere models should prove useful in examining air-sea causal mechanisms creating the persistence in regional ice and atmospheric parameters, as well as in evaluating potential predictability of the Odden.

[18] **Acknowledgments.** We thank Sheng-Hung Wang, Lin Li, and Lei Yang of the Byrd Polar Research Center for computer program support and we thank the reviewers of this paper for helpful comments. This research work is supported by NSF Office of Polar Programs research grant ARC-0629338.

References

Chasmer, L. E., and E. F. LeDrew (2001), Weekly interactions between sea ice concentrations and the North Atlantic oscillation in the Odden sea ice peninsula, Greenland Sea, in *IEEE International Geoscience and Remote Sensing Symposium*, vol. 3, pp. 1249–1251, Inst. of Eng. and Technol., London.

Comiso, J. C., P. Wadhams, L. T. Pedersen, and R. A. Gersten (2001), Seasonal and interannual variability of the Odden ice tongue and a study of environmental effects, *J. Geophys. Res.*, *106*, 9093–9116.

Deser, C., J. E. Walsh, and M. S. Timlin (2000), Arctic sea ice variability in the context of recent atmospheric circulation trends, *J. Clim.*, *13*, 617–633.

Dickson, R. R., J. Meincke, S. A. Malmberg, and A. J. Lee (1988), The "great salinity anomaly" in the northern North Atlantic 1968–1982, *Prog. Oceanogr.*, *20*, 103–151.

Dickson, R. R., et al. (2000), The Arctic Ocean response to the North Atlantic Oscillation, *J. Clim.*, *13*, 2671–2696.

Kalnay, E., et al. (1996), The NCEP/NCAR 40-year reanalysis project, *Bull. Am. Meteorol. Soc.*, *77*, 437–471.

Rayner, N. A., D. E. Parker, E. B. Horton, C. K. Folland, L. V. Alexander, D. P. Rowell, E. C. Kent, and A. Kaplan (2003), Global analyses of sea surface temperature, sea ice, and night marine air temperature since the late nineteenth century, *J. Geophys. Res.*, *108*(D14), 4407, doi:10.1029/2002JD002670.

Rogers, J. C. (1984), The association between the North Atlantic Oscillation and the Southern Oscillation in the Northern Hemisphere, *Mon. Weather Rev.*, *112*, 1999–2015.

Rogers, J. C., C.-C. Wang, and M. McHugh (1998), Persistent cold climatic episodes around Greenland and Baffin Island: Links to decadal-scale sea surface temperature anomalies, *Geophys. Res. Lett.*, *25*, 3971–3974.

Shuchman, R. A., E. G. Josberger, C. A. Russel, K. W. Fischer, O. M. Johannessen, J. Johannessen, and P. Gloersen (1998), Greenland Sea Odden sea ice feature: Intra-annual and interannual variability, *J. Geophys. Res.*, *103*, 12,709–12,724.

Toudal, L. (1999), Ice extent in the Greenland Sea 1978–1995, *Deep Sea Res., Part II*, *46*, 1237–1254.

Toudal, L., and M. D. Coon (2001), Interannual variability of the sea-ice induced salt flux in the Greenland Sea, *Ann. Glaciol.*, *33*, 385–390.

Visbeck, M., J. Fischer, and F. Schott (1995), Preconditioning the Greenland Sea for deep convection: Ice formation and ice drift, *J. Geophys. Res.*, *100*, 18,489–18,502.

Wadhams, P., and J. C. Comiso (1999), Two modes of appearance of the Odden ice tongue in the Greenland Sea, *Geophys. Res. Lett.*, *26*, 2497–2500.

Walsh, J. E. (1978). A data set on Northern Hemisphere sea ice extent, 1953–1976, Arctic Sea Ice, part 1, *Glaciol. Data Rep. GD-2*, http://www.cgd.ucar.edu/cas/guide/Data/walsh.html, pp. 49–51, World Data Cent. for Glaciol. [Snow and Ice], Boulder, Colo.

M.-P. Hung and J. C. Rogers, Atmospheric Science Program, Department of Geography, Ohio State University, 1036 Derby Hall, Columbus, OH 43210-1361, USA. (hung.84@osu.edu; rogers.21@osu.edu)